ACS APPLIED MATERIALS & INTERFACES

Research Article

www.acsami.org

High Areal Capacity Hybrid Magnesium–Lithium-Ion Battery with 99.9% Coulombic Efficiency for Large-Scale Energy Storage

Hyun Deog Yoo,[†] Yanliang Liang,[†] Yifei Li,[†] and Yan Yao*[,†,‡]

[†]Department of Electrical and Computer Engineering and Materials Science and Engineering Program, University of Houston, Houston, Texas 77204, United States

[‡]Texas Center for Superconductivity, University of Houston, Houston, Texas 77204, United States

Supporting Information

ABSTRACT: Hybrid magnesium–lithium-ion batteries (MLIBs) featuring dendrite-free deposition of Mg anode and Li-intercalation cathode are safe alternatives to Li-ion batteries for large-scale energy storage. Here we report for the first time the excellent stability of a high areal capacity MLIB cell and dendrite-free deposition behavior of Mg under high current density (2 mA cm^{-2}). The hybrid cell showed no capacity loss for 100 cycles with Coulombic efficiency as high as 99.9%, whereas the control cell with a Li-metal anode only retained 30% of its original capacity with Coulombic efficiency well below 90%. The use of TiS_2 as a cathode enabled the highest specific capacity and one of the best rate performances among reported MLIBs. Postmortem analysis of the cycled cells revealed dendrite-free Mg deposition on a Mg anode surface, while mossy Li dendrites were observed covering the Li surface and penetrated into separators in the Li cell. The energy density of a MLIB could be further improved by developing electrolytes with higher salt concentration and wider electrochemical window, leading to new opportunities for its application in large-scale energy storage.

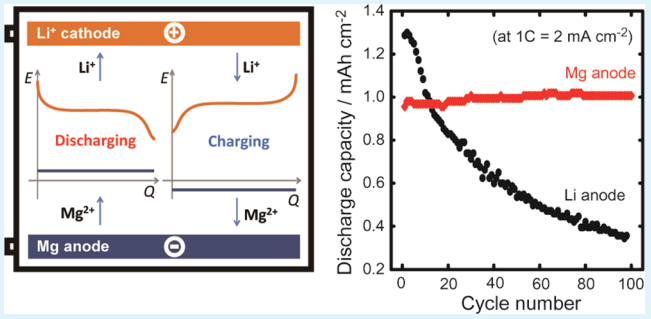

KEYWORDS: *hybrid magnesium–lithium-ion batteries (MLIBs), energy storage, Coulombic efficiency, dendrite-free magnesium deposition*

INTRODUCTION

Development of safe and high-energy rechargeable batteries has been driven by the growing demands of large-scale energy storage.[1] Li–oxygen and Li–sulfur batteries have received significant attention in recent years due to their ultra-high-energy density.[2] However, these Li-metal-based batteries suffer from safety challenges related to dendritic Li growth, which often leads to internal short circuit and thermal runaway.[3−5] Many approaches have been developed to suppress the formation of dendrites on a Li-metal surface and we have seen significant progress in recent years.[6−11] Nevertheless, dendrite formation is still a detrimental issue, in particular, at high-rate charging conditions (1−2 mA cm^{-2}) that limit the cycle life of Li-metal batteries within 150 cycles.[6] On the other hand, magnesium rechargeable batteries (MgRBs) excel in safety features thanks to the highly reversible deposition and dissolution of metallic Mg anode.[12−16] Mg-metal anode is resistant to dendrite formation due to (1) the unique electrodeposition behavior that Mg favors planar hexagonal growth and (2) the strong nucleophilic nature of Mg electrolyte that keeps the metal–electrolyte interface free from passivation films.[17−19] However, the challenge for MgRBs is the lack of suitable high-capacity cathode materials caused by the slow solid-state diffusion of highly polarizing divalent Mg ions in most intercalation hosts.[20−22]

While both lithium rechargeable batteries (LiRBs) and MgRBs have their limitations, a hybrid magnesium–lithium-ion battery (MLIB) that combines a stable Mg-metal anode and a fast Li-intercalation cathode can offer significant advantages in terms of safety and stability.[23−25] The working principle of a MLIB is shown in Figure 1a. Because the thermodynamic redox potential of Mg^{2+}/Mg is 0.67 V higher than that of Li^+/Li, reversible Mg deposition/dissolution occurs at the anode side before Li deposition/dissolution could take place. On the cathode side, Li^+ ion dominates intercalation because Mg^{2+} diffuses several orders of magnitude slower compared to Li^+ in the same host materials. Because of the asymmetric use of Mg^{2+} and Li^+ on each side of electrodes, the hybrid electrolyte has to be an ion reservoir that could supply enough Li^+ and receive Mg^{2+} during discharge, and vice versa during charge. The maximum energy density (E_v, Wh L^{-1}) of a MLIB can be represented as

$$E_v = zFVc/3600 \quad (1)$$

where z is the number of charge for the intercalated ion (1 for Li^+), F is the Faraday constant (96 485 C mol^{-1}), V is the

Received: February 6, 2015
Accepted: March 17, 2015
Published: March 23, 2015

DOI: 10.1021/acsami.5b01206
ACS Appl. Mater. Interfaces 2015, 7, 7001−7007

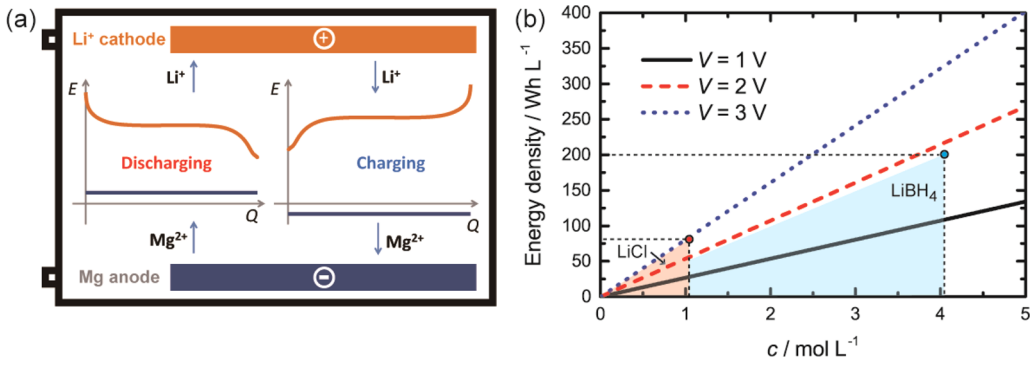

Figure 1. (a) Schematic illustration of the working mechanism of a hybrid MLIB. The cell is discharged with simultaneous Li^+ intercalation into the cathode and Mg^{2+} dissolution from the anode. Upon charging, Li^+ is deintercalated from the cathode while Mg is deposited on the anode. Corresponding voltage profiles of both electrodes are represented in orange and blue lines, respectively. (b) The maximum energy density of a hybrid MLIB dependence on ion concentration (c) as well as the electrochemical window of electrolyte (V). When LiCl is used as Li-ion source, the highest energy density is 80 Wh L^{-1} (red dot), while when $LiBH_4$ is used, the highest energy density is 200 Wh L^{-1} (blue dot).

voltage window of the electrolyte (V), and c is the concentration of Li^+ in the hybrid electrolyte (mol L^{-1}). As shown in Figure 1b, the hybrid electrolyte plays an important role in determining the maximum energy density of a MLIB cell: the higher the Li-ion concentration and the wider electrochemical window of the electrolyte, the higher the maximum energy density one can achieve. Since most MLIBs developed so far utilize either lithium chloride (LiCl) or lithium borohydride ($LiBH_4$) as the Li source, we added these two cases in Figure 1b. LiCl salt could enable a 3 V (vs Mg^{2+}/Mg) electrochemical window while its solubility is limited to 1 M in ether solvents; thus, the maximum energy density is 80 Wh L^{-1} (orange region). $LiBH_4$ could provide higher energy density up to 200 Wh L^{-1} (blue region) due to higher solubility up to 4 M in diglyme but with a reduced electrochemical window of only 1.8 V (vs Mg^{2+}/Mg). This analysis shows that MLIBs could potentially compete with Pb-acid batteries (60−75 Wh L^{-1}) and Ni−Cd (50−150 Wh L^{-1}) for large-scale energy storage when being fully optimized.

Chevrel phase molybdenum sulfide (Mo_6S_8),[23,25−27] lithium-metal phosphates,[24,28] (lithium)-metal oxides,[13,29,30] and titanium disulfide (TiS_2)[31] have been investigated as cathode materials in MLIBs. All previous works have focused on either cathode selection or electrolyte optimization with relatively low areal capacity of 0.1−0.6 mAh cm^{-2} (Table S1), under which the Mg-metal anode surface is almost kept intact even after repeated hundreds of cycles. To directly compare with Li-metal-based cells which only fails quickly at high areal capacity and high current conditions,[6,8] it is important to test a MLIB in similar conditions to demonstrate its full potential.

Here we report for the first time the excellent stability of a high areal capacity MLIB cell and dendrite-free deposition behavior of Mg under high current density (2 mA cm^{-2}). The hybrid cell showed stable cycling without capacity loss for the first 100 cycles while a Li-metal anode retained only 30% of the original capacity during the same cycles. The Coulombic efficiency of the MLIB cell was as high as 99.9%, whereas the Coulombic efficiency of the control cell was well below 90%. Analysis of the cycled cells revealed polyhedral Mg deposits on the Mg anode surface while in control cells mossy Li dendrites loosely cover the Li surface and penetrate the separators.

EXPERIMENTAL SECTION

Preparation of Electrodes. Titanium disulfide (TiS_2, 99.8%, Strem Chemicals Inc., Newburyport, MA) was used as purchased. A slurry of active material (80 wt %), Super-P carbon (10 wt %), and polyvinylidene fluoride (10 wt %) dispersed in *N*-methyl-2-pyrrolidone was spread on a piece of stainless steel mesh (0.8 cm^2) and dried as the working electrode. Mass loading of the active material was 0.3−0.6 mg cm^{-2} for electrochemical characterizations and 7.5−8.5 mg cm^{-2} for high areal capacity cells. Freshly polished magnesium foil (50 μm thick, 99.95%, GalliumSource, LLC, Scotts Valley, CA) was used as both the counter and reference electrodes.

Preparation of Electrolytes. All-phenyl complex (APC) electrolyte, a solution of 0.25 M $[Mg_2Cl_3]^+[AlPh_2Cl_2]^-$ in tetrahydrofuran (THF, Sigma-Aldrich Co., St. Louis, MO), was prepared following Aurbach and co-workers[32,33] and served as the Mg-ion electrolyte. Li^+/Mg^{2+} hybrid-ion electrolyte was prepared by adding 0.5 M lithium chloride (LiCl, 99.9%, Alfa-Aesar Co., Ward Hill, MA) into the APC electrolyte. For hybrid cells with high areal capacity (1.9 mAh cm^{-2}), 1 M LiCl was added into the APC electrolyte. Lithium perchlorate (1 M $LiClO_4$) in THF or a mixture of ethylene-carbonate (EC) and diethyl-carbonate (DEC) with 1:1 volumetric ratio was used as Li-ion electrolyte.

Electrochemical and Microscopic Characterizations. Tubular hermetically sealed three-electrode cells or CR2032 coin-type cells were fabricated for electrochemical characterizations. The cells were assembled in an Ar-filled glovebox (M-Braun Co., Garching, Germany). For coin cells, two separators were placed between two electrodes in the following sequence: a metal anode, a glass fiber separator (210 μm thick, VWR grade 691), a trilayer polypropylene/polyethylene/polypropylene (PP/PE/PP) separator (25 μm thick, Celgard 2325, Celgard, LLC, Charlotte, NC), and a cathode. The three-electrode and two-electrode cell characterizations were conducted using a potentiostat (VMP-3, Bio-Logic Co., Claix, France) and battery cycler (CT2001A, LANHE, Wuhan, China). The electrodes and separators were characterized by a scanning electron microscope (SEM, LEO Gemini 1525, ZWL, Lauf a. d. Pegnitz, Germany).

RESULTS AND DISCUSSION

The selection of a suitable Mg-ion electrolyte and Li-ion salt for a hybrid-ion electrolyte is critical for proper battery operation.

DOI: 10.1021/acsami.5b01206
ACS Appl. Mater. Interfaces 2015, 7, 7001−7007

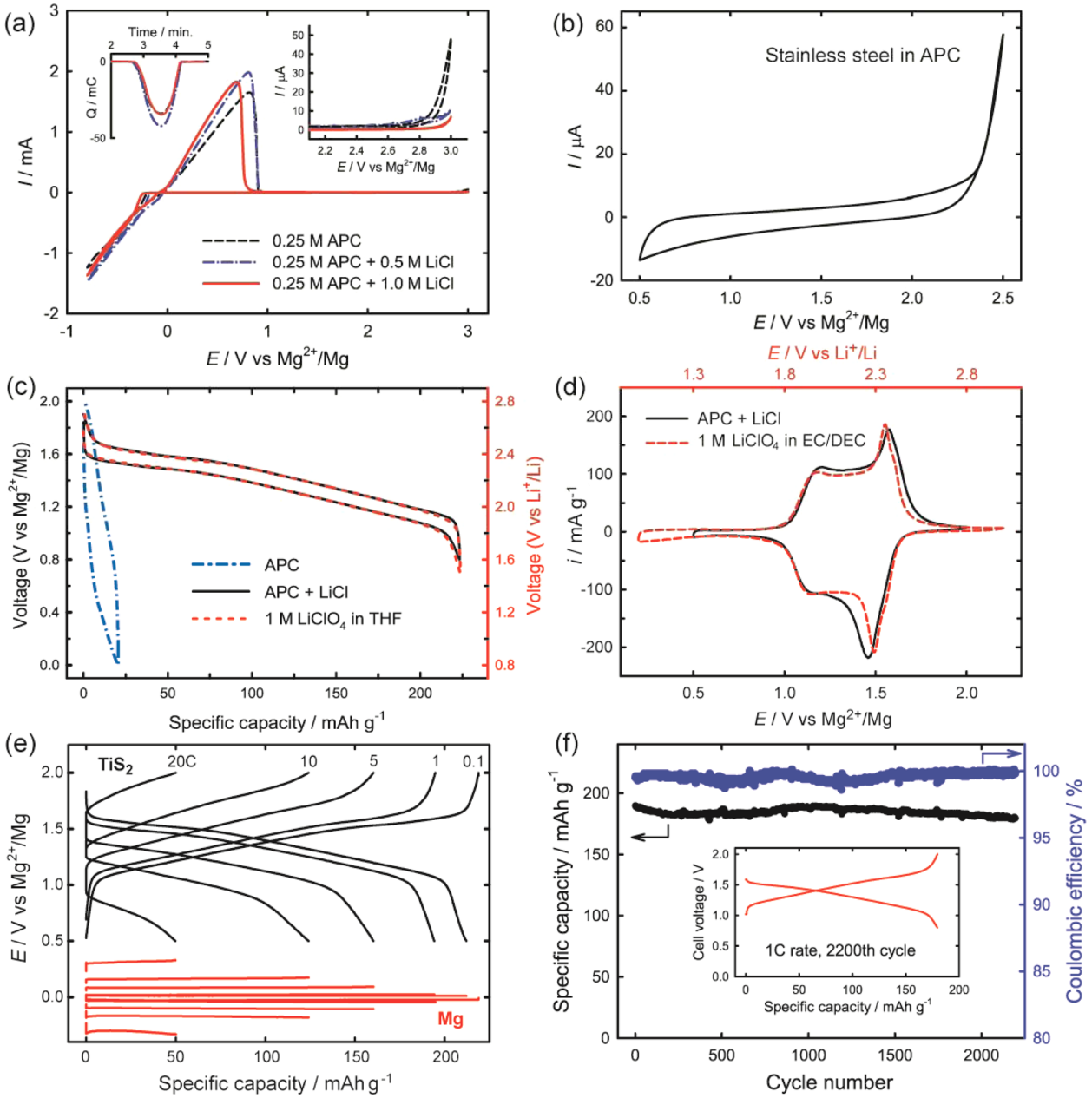

Figure 2. A hybrid MLIB using a Mg-metal anode and a TiS_2 cathode. (a) Cyclic voltammograms of three electrolyte configuration at 25 mV s^{-1} scan rate. 0.25 M APC solution with 0.0, 0.5, and 1.0 M LiCl as additive with platinum wire as the working electrode. (b) Cyclic voltammogram of a stainless steel substrate in 0.25 M APC electrolyte. (c) Voltage profiles of TiS_2 electrode in APC solution with or without 0.5 M LiCl and 1 M $LiClO_4$ in THF electrolytes during 0.1C charge−discharge. (d) Cyclic voltammograms obtained from three-electrode cells comprising TiS_2 as the working electrode and Mg or Li as reference and counter electrodes (scan rate = 0.1 mV s^{-1}). (e) Voltage profiles for the TiS_2 cathode (black lines) and Mg anode (red lines) in a hybrid MLIB at different C rate. (f) Cycling performance of a MLIB cell over 2000 cycles at 1C rate. 1C = 0.241 A g^{-1}.

Standard all-phenyl complex (APC) electrolyte, 0.25 M $Mg_2Cl_3^+AlPh_2Cl_2^-$ in tetrahydrofuran (THF),[33] was used due to its capability to reversibly deposit and dissolute Mg with 100% Coulombic efficiency (Figure 2a) and stable electrochemical window up to 2.3 V vs Mg^{2+}/Mg on stainless steel substrates (Figure 2b). LiCl salt was added into the APC electrolyte because Cl^- anion prevents formation of passivation film on a Mg surface.[13,34] Two different concentrations of LiCl (0.5−1.0 M) were added into APC electrolyte. In agreement with previous studies,[23,34] the anodic stability was slightly enhanced with the addition of LiCl (Figure 2a). The overpotential for Mg deposition was lowered to 130 mV at 0.5 M LiCl addition in comparison to the overpotential of 155 mV without additive. Coulombic efficiency of Mg deposition/dissolution was slightly lowered to 99.3−99.6% with the addition of LiCl (inset of Figure 2a and Table S2 of the Supporting Information). Overall, there is no significant changes in the performance of Mg anode when LiCl was added, which is important to ensure proper operation of a MLIB.

As the first reported Li-ion intercalation cathode, TiS_2-based electrodes demonstrated capacity as high as 220 mAh g^{-1} in pure Li-ion electrolyte.[35] However, it is a poor cathode in its pristine form for Mg-ion intercalation due to the sluggish kinetics of Mg ion in TiS_2.[36] Figure 2c shows the specific capacity of TiS_2 electrode less than 20 mAh g^{-1} in pure APC

DOI: 10.1021/acsami.5b01206
ACS Appl. Mater. Interfaces 2015, 7, 7001−7007

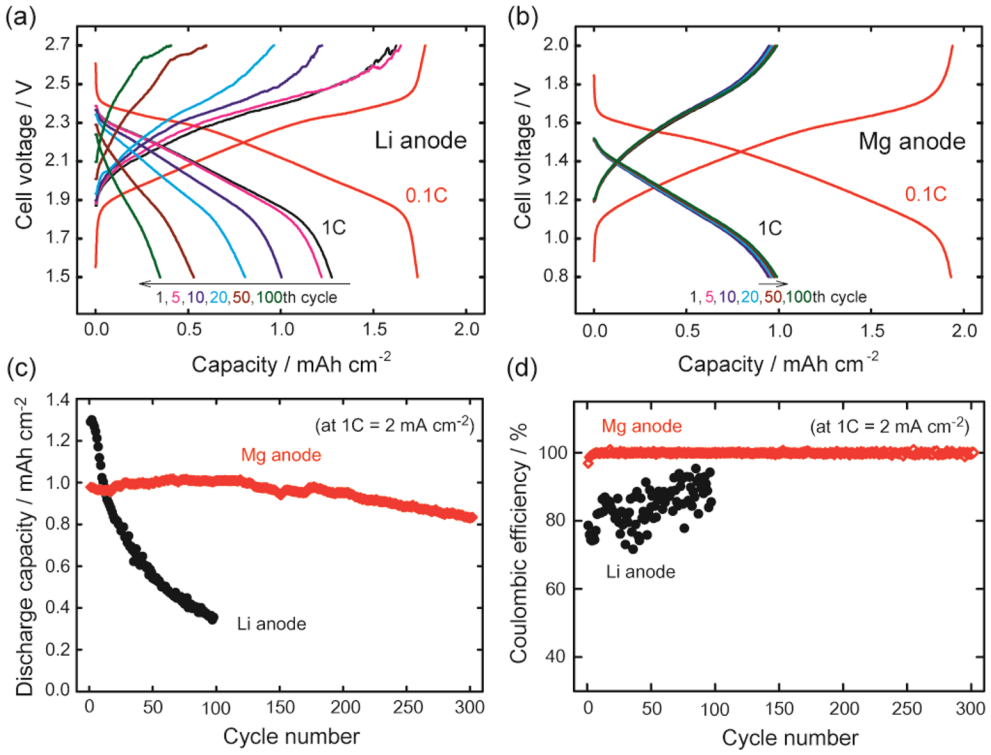

Figure 3. Electrochemical performance comparison for two cells with practical-level areal capacity with the active material TiS_2 mass loading to 8.0 ± 0.5 mg cm^{-2}. Voltage profiles of (a) Li-anode cell and (b) a MLIB. 1C = 2 mA cm^{-2}, 0.1C = 0.2 mA cm^{-2}. Comparison of (c) discharge capacity and (d) Coulombic efficiency for 300 cycles.

electrolyte. However, the capacity could increase to 220 mAh g^{-1} in Li^+/Mg^{2+} hybrid electrolyte or in pure Li electrolyte. As shown in Figure 2d, similar shape of cyclic voltammograms (CV) curves in both electrolytes confirms that Li^+ intercalation dominates the cathode reaction in MLIB. The 0.8 V difference in redox potentials can be ascribed to the different potentials of Li and Mg used as the reference electrodes. The rate performance of the MLIB cell was tested in a three-electrode setup (Figure 2e). At 0.1C rate, the cell shows specific capacity of 220 mAh g^{-1} and average discharge voltage of 1.4 V. The specific energy of 308 Wh kg^{-1} is the highest ever reported in MLIBs (see Table S1 for comparison). The specific capacity reduces to 195 mAh g^{-1} at 1C, 125 mAh g^{-1} at 10C, and retains 50 mAh g^{-1} even at 20C. This excellent rate performance is related to the fast diffusion kinetics of Li ions in TiS_2 cathode. The overpotential for Mg dissolution was 10, 30, 170, and 330 mV at 0.1C, 1C, 10C, and 20C, respectively (Figure 2e). The hybrid MLIB was cycled at 1C for over 2000 cycles with less than 5% capacity decay (Figure 2f). The average Coulombic efficiency was 99.6 ± 0.2% during the 2000 cycles.

With the keen interests of studying MLIBs at high current density and high areal capacity, we intentionally increased the active material mass loading to 8.0 ± 0.5 mg cm^{-2}. We fabricated a MLIB and a Li|TiS_2 cell with similar mass loading for side-by-side comparison. When the two cells were cycled at low rate (0.2 mA cm^{-2}), both cells showed similar capacity (Figure 3a,b). However, when the current was increased to 2 mA cm^{-2}, we observed a drastic difference in performance. For the Li|TiS_2 cell, the capacity decreased severely from 1.3 to 0.4 mAh cm^{-2} during 100 cycles (Figure 3c) and the Coulombic efficiency was consistently lower than 90% (Figure 3d). This observation is consistent with previous reports that Li dendrite formation limits the cycle life of Li-metal batteries at high-rate charging (1−2 mA cm^{-2}).[6] In comparison, the hybrid MLIB cell showed no capacity loss for the first 100 cycles and 80% capacity retention for a total of 300 cycles (Figure 3c). Figure 3d shows the Coulombic efficiency of 99.9 ± 0.3% throughout the 300 cycles. The statistics of the Coulombic efficiency data are shown in Figure S1. We note the initial lower capacity of the MLIB cell (1.0 mAh cm^{-2}) compared to that of the Li|TiS_2 cell (1.3 mAh cm^{-2}) is coming from the higher overpotential of Mg anodes and the lower ionic conductivity of MLIB electrolyte (~3 mS cm^{-1}) compared to that of the Li^+ electrolyte (4.8 mS cm^{-1}).[18,32,37]

To explore the origin of capacity fading in the Li|TiS_2 cell at 1C rate, we compared three configurations: a two-electrode coin cell with high mass loading (1.3 mAh cm^{-2}), a two-electrode cell with low mass loading (0.2 mAh cm^{-2}), and a three-electrode tube cell with high mass loading (0.9 mAh cm^{-2}). As shown in Figure 4a, the capacity decay was not observed in the latter two configurations, leading us to confirm the hypothesis that the capacity decay in the Li|TiS_2 cell is due to the failure of Li anode instead of the degradation of TiS_2 cathode. Indeed, the transparent tube cell in Figure 4b allowed us to observe the dendritic growth of Li. However, the sufficient distance between the electrodes prevents the dendrite growth to touch the counter electrode. The stable capacity cycling of the three-electrode tube cell indicates the TiS_2 cathode does not degrade in such a three-electrode configuration. However, the scenario becomes very different in the case of two-electrode coin cell with high mass loading. Figure 5a,b shows the glass fiber separator penetrated by metallic dark brown powders, which were later identified to be Li particles (Figure S2). The Li powders were partially infiltrated into the PP/PE/PP separator next to the cathode side (Figure S3). From the SEM cross-sectional image in Figure

DOI: 10.1021/acsami.5b01206
ACS Appl. Mater. Interfaces 2015, 7, 7001−7007

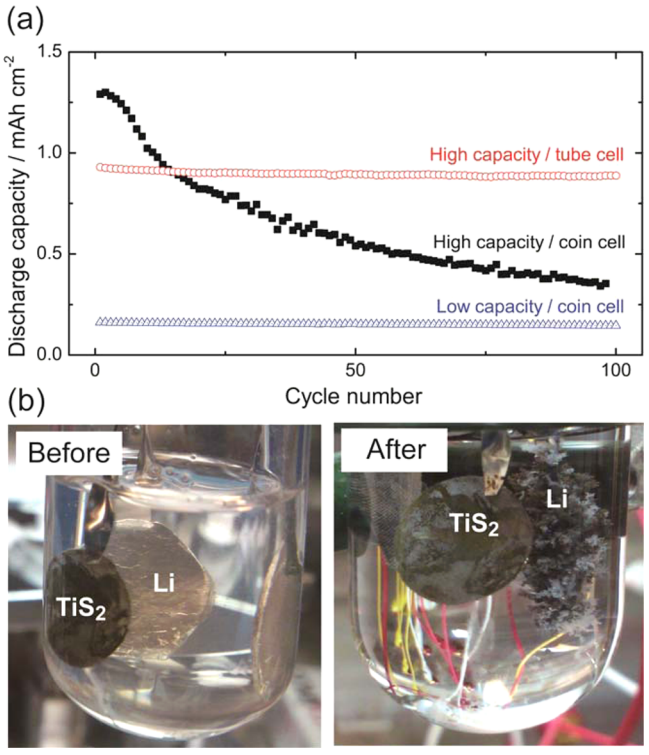

Figure 4. (a) Cycling performance of Li|TiS$_2$ cells at 1C rate charge–discharge with three different configurations: a two-electrode coin cell (0.2 mAh cm^{-2}, blue), a two-electrode coin cell (1.3 mAh cm^{-2}, black), and a three-electrode tube cell (0.9 mAh cm^{-2}, red). (b) Optical images of the three-electrode tube cell before and after six cycles at 1C rate (1.2 mA cm^{-2}).

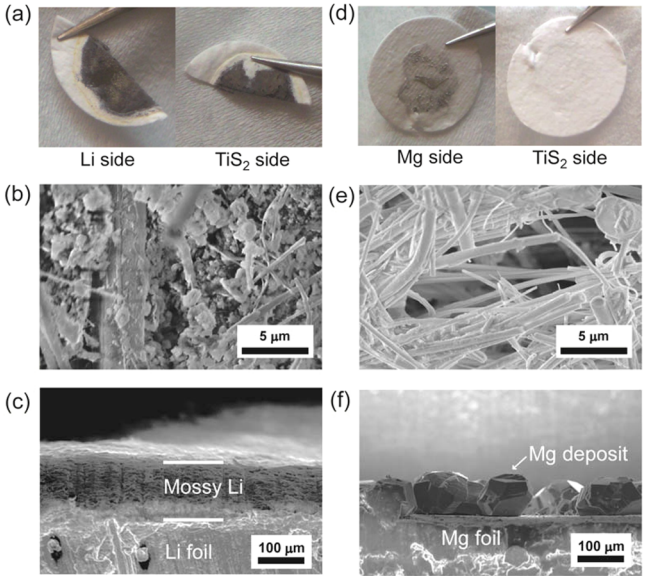

Figure 5. Optical and SEM images of separators and metal anodes for Li- and Mg-metal-based cells after 100 and 300 high current cycles, respectively. Optical images for both sides of glass fiber separators in (a) a Li battery and (d) a hybrid MLIB. Cross-sectional SEM images of glass fiber separators in (b) a Li battery and (e) a hybrid MLIB. Cross-sectional SEM images of (c) Li-metal anode and (f) Mg-metal anode.

5c, we observed the Li anode was covered with a 100 μm thick mossy layer composed of the mixture of dead Li particles and solid electrolyte interphase (SEI). Taking all this evidence into consideration, we conclude that dendritic growth of Li anode is the origin of capacity fading in the Li|TiS$_2$ cell.

To obtain direct evidence of dendrite-free Mg deposition in the MLIB cell, we did postmortem analysis for the cell after 300 cycles and conducted optical and microscopic characterizations. As shown in Figure 5d, the glass fiber separator was as clean as the original (only a little Mg debris attached to one side of the separator). We cut the separator open and checked the inner part of the separator and found no Mg particles (Figure 5e). The cross-sectional SEM of the Mg anode in Figure 5f reveals single-layer polyhedral Mg deposits due to the hexagonal closed packed (hcp) structure of Mg metal. The prolonged cycling at high current density leads to the growth of Mg crystals to an average size around 100 μm. This finding suggests that we may need to use a separator with sufficient thickness for long-term high rate cycling even though the Mg deposition is non-dendritic. Overall, these characterizations testify that Mg deposition is nondendritic in nature and thus enables highly reversible and stable anode operation in MLIBs.

Several directions could be further explored to increase the energy density of MLIBs. According to eq 1, the maximum energy density is linearly proportional to the electrolyte voltage window; recently developed electrolytes with wider stability window will significantly broaden the choice of cathode materials with higher redox potentials.[29,38] Also, employing Li source with higher solubility in electrolyte will effectively improve the energy density of MLIBs. Electrolytes saturated with Li salts[24] or solvent-in-salt electrolytes[25,39] are promising candidates for such purposes. For practical considerations, glyme ($CH_3O(C_2H_4O)_nCH_3$, n = 1–4) based solvents with higher boiling point and lower vapor pressure are preferred to replace the volatile THF solvent.[26,30,36]

CONCLUSIONS

In summary, excellent stability for a high areal capacity MLIB cell and nondendritic deposition behavior of Mg were demonstrated under high current density. The use of TiS$_2$ as cathode achieved the highest specific capacity in MLIBs as well as excellent cycling stability. The hybrid cell showed significantly better capacity retention and higher Coulombic efficiency compared to the control cell with Li-metal anode. Analysis of the cycled Li|TiS$_2$ cell led us to conclude that the dendritic growth of Li anode instead of the degradation of TiS$_2$ cathode is responsible for the capacity fading. The key advantages of operating MLIBs under practical high current and high areal capacity conditions are unambiguously demonstrated. The energy density of MLIBs can be further improved with optimized hybrid electrolyte, which will open up new opportunities for the development of advanced materials for large-scale energy storage.

ASSOCIATED CONTENT

Supporting Information

Detailed electrochemical and optical measurements. This material is available free of charge via the Internet at http://pubs.acs.org.

AUTHOR INFORMATION

Corresponding Author

*E-mail: yyao4@uh.edu.

DOI: 10.1021/acsami.5b01206
ACS Appl. Mater. Interfaces 2015, 7, 7001–7007

Notes

The authors declare no competing financial interest.

■ ACKNOWLEDGMENTS

We acknowledge financial support through the U.S. Office of Naval Research Award (No. N00014-13-1-0543) and the startup fund from Cullen College of Engineering at the University of Houston.

■ REFERENCES

(1) Dunn, B.; Kamath, H.; Tarascon, J.-M. Electrical Energy Storage for the Grid: a Battery of Choices. *Science* **2011**, *334* (6058), 928−935.
(2) Bruce, P. G.; Freunberger, S. A.; Hardwick, L. J.; Tarascon, J.-M. Li-O_2 and Li-S Batteries with High Energy Storage. *Nat. Mater.* **2012**, *11* (1), 19−29.
(3) Gofer, Y.; Ben-Zion, M.; Aurbach, D. Solutions of $LiAsF_6$ in 1,3-Dioxolane for Secondary Lithium Batteries. *J. Power Sources* **1992**, *39* (2), 163−178.
(4) Tarascon, J.-M.; Amatucci, G. G. Rechargeable Li-ion Batteries for Satellite Applications: Pros and Cons. In *Microengineering Aerospace Systems*, Helvajian, H., Ed.; The Aerospace Press: El Segundo, CA, 1999; Chapter 6, pp 201−226.
(5) Goodenough, J. Rechargeable Batteries: Challenges Old and New. *J. Solid State Electrochem.* **2012**, *16* (6), 2019−2029.
(6) Aurbach, D.; Zinigrad, E.; Teller, H.; Dan, P. Factors Which Limit the Cycle Life of Rechargeable Lithium (Metal) Batteries. *J. Electrochem. Soc.* **2000**, *147* (4), 1274−1279.
(7) Zhang, S. S.; Xu, K.; Jow, T. R. Study of the Charging Process of a $LiCoO_2$-Based Li-Ion Battery. *J. Power Sources* **2006**, *160* (2), 1349−1354.
(8) Lu, D.; Shao, Y.; Lozano, T.; Bennett, W. D.; Graff, G. L.; Polzin, B.; Zhang, J.; Engelhard, M. H.; Saenz, N. T.; Henderson, W. A.; Bhattacharya, P.; Liu, J.; Xiao, J. Failure Mechanism for Fast-Charged Lithium Metal Batteries with Liquid Electrolytes. *Adv. Energy Mater.* **2015**, *5* (3), 1400993.
(9) Ansari, Y.; Guo, B.; Cho, J. H.; Park, K.; Song, J.; Ellison, C. J.; Goodenough, J. B. Low-Cost, Dendrite-Blocking Polymer-Sb_2O_3 Separators for Lithium and Sodium Batteries. *J. Electrochem. Soc.* **2014**, *161* (10), A1655−A1661.
(10) Huang, C.; Xiao, J.; Shao, Y.; Zheng, J.; Bennett, W. D.; Lu, D.; Saraf, L. V.; Engelhard, M.; Ji, L.; Zhang, J.; Li, X.; Graff, G. L.; Liu, J. Manipulating Surface Reactions in Lithium−Sulphur Batteries Using Hybrid Anode Structures. *Nat. Commun.* **2014**, *5*, 3015.
(11) Zheng, G.; Lee, S. W.; Liang, Z.; Lee, H.-W.; Yan, K.; Yao, H.; Wang, H.; Li, W.; Chu, S.; Cui, Y. Interconnected Hollow Carbon Nanospheres for Stable Lithium Metal Anodes. *Nat. Nanotechnol.* **2014**, *9*, 618−623.
(12) Muldoon, J.; Bucur, C. B.; Oliver, A. G.; Sugimoto, T.; Matsui, M.; Kim, H. S.; Allred, G. D.; Zajicek, J.; Kotani, Y. Electrolyte Roadblocks to a Magnesium Rechargeable Battery. *Energy Environ. Sci.* **2012**, *5* (3), 5941−5950.
(13) Yoo, H. D.; Shterenberg, I.; Gofer, Y.; Gershinsky, G.; Pour, N.; Aurbach, D. Mg Rechargeable Batteries: an On-going Challenge. *Energy Environ. Sci.* **2013**, *6*, 2265−2279.
(14) Mohtadi, R.; Mizuno, F. Magnesium Batteries: Current State of the Art, Issues and Future Perspectives. *Beilstein J. Nanotechnol.* **2014**, *5*, 1291−1311.
(15) Saha, P.; Datta, M. K.; Velikokhatnyi, O. I.; Manivannan, A.; Alman, D.; Kumta, P. N. Rechargeable Magnesium Battery: Current Status and Key Challenges for the Future. *Prog. Mater. Sci.* **2014**, *66*, 1−86.
(16) Muldoon, J.; Bucur, C. B.; Gregory, T. Quest for Nonaqueous Multivalent Secondary Batteries: Magnesium and Beyond. *Chem. Rev.* **2014**, *114* (23), 11683−11720.
(17) Ling, C.; Banerjee, D.; Matsui, M. Study of the Electrochemical Deposition of Mg in the Atomic Level: Why It Prefers the Non-dendritic Morphology. *Electrochim. Acta* **2012**, *76*, 270−274.
(18) Matsui, M. Study on Electrochemically Deposited Mg Metal. *J. Power Sources* **2011**, *196* (16), 7048−7055.
(19) Jäckle, M.; Groß, A. Microscopic Properties of Lithium, Sodium, and Magnesium Battery Anode Materials Related to Possible Dendrite Growth. *J. Chem. Phys.* **2014**, *141*, 174710.
(20) Amatucci, G. G.; Badway, F.; Singhal, A.; Beaudoin, B.; Skandan, G.; Bowmer, T.; Plitza, I.; Pereira, N.; Chapman, T.; Jaworski, R. Investigation of Yttrium and Polyvalent Ion Intercalation into Nanocrystalline Vanadium Oxide. *J. Electrochem. Soc.* **2001**, *148* (8), A940−A950.
(21) Liang, Y.; Yoo, H. D.; Li, Y.; Shuai, J.; Calderon, H. A.; Robels Hernandez, F. C.; Grawbow, L. C.; Yao, Y. Interlayer-Expanded Molybdenum Disulfide Nanocomposites for Electrochemical Magnesium Storage. *Nano Lett.* **2015**, *15* (3), 2194−2202.
(22) Wu, N.; Yin, Y.-X.; Guo, Y.-G. Size-Dependent Electrochemical Magnesium Storage Performance of Spinel Lithium Titanate. *Chem.—Asian J.* **2014**, *9* (8), 2099−2102.
(23) Gofer, Y.; Chusid, O.; Gizbar, H.; Viestfrid, Y.; Gottlieb, H. E.; Marks, V.; Aurbach, D. Improved Electrolyte Solutions for Rechargeable Magnesium Batteries. *Electrochem. Solid-State Lett.* **2006**, *9* (5), A257−A260.
(24) Yagi, S.; Ichitsubo, T.; Shirai, Y.; Yanai, S.; Doi, T.; Murase, K.; Matsubara, E. A Concept of Dual-Salt Polyvalent-Metal Storage Battery. *J. Mater. Chem. A* **2014**, *2* (4), 1144−1149.
(25) Cheng, Y.; Shao, Y.; Zhang, J.-g.; Sprenkle, V. L.; Liu, J.; Li, G. High Performance Batteries Based on Hybrid Magnesium and Lithium Chemistry. *Chem. Commun.* **2014**, *50*, 9644−9646.
(26) Shao, Y.; Liu, T.; Li, G.; Gu, M.; Nie, Z.; Engelhard, M.; Xiao, J.; Lv, D.; Wang, C.; Zhang, J.-G.; Liu, J., Coordination Chemistry in Magnesium Battery Electrolytes: How Ligands Affect Their Performance. *Sci. Rep.* **2013**, *3*.
(27) Cho, J.-H.; Aykol, M.; Kim, S.; Ha, J.-H.; Wolverton, C.; Chung, K. Y.; Kim, K.-B.; Cho, B.-W. Controlling the Intercalation Chemistry to Design High-Performance Dual-Salt Hybrid Rechargeable Batteries. *J. Am. Chem. Soc.* **2014**, *136* (46), 16116−16119.
(28) Gofer, Y.; Pour, N.; Aurbach, D. Electrolytic Solutions for Rechargeable Magnesium Batteries. In *Lithium Batteries*; John Wiley & Sons, Inc.: New York, 2013; pp 327−347.
(29) Nelson, E. G.; Brody, S. I.; Kampf, J. W.; Bartlett, B. M. A Magnesium Tetraphenylaluminate Battery Electrolyte Exhibits a Wide Electrochemical Potential Window and Reduces Stainless Steel Corrosion. *J. Mater. Chem. A* **2014**, *2* (43), 18194−18198.
(30) Su, S.; Huang, Z.; NuLi, Y.; Tuerxun, F.; Yang, J.; Wang, J. A Novel Rechargeable Battery with a Magnesium Anode, a Titanium Dioxide Cathode, and a Magnesium Borohydride/Tetraglyme Electrolyte. *Chem. Commun.* **2015**, *51*, 2641−2644.
(31) Gao, T.; Han, F.; Zhu, Y.; Suo, L.; Luo, C.; Xu, K.; Wang, C. Hybrid Mg^{2+}/Li^+ Battery with Long Cycle Life and High Rate Capability. *Adv. Energy Mater.* **2015**, *5* 5, 1401507.
(32) Yoo, H. D.; Shterenberg, I.; Gofer, Y.; Doe, R. E.; Fischer, C. C.; Ceder, G.; Aurbach, D. A Magnesium-Activated Carbon Hybrid Capacitor. *J. Electrochem. Soc.* **2014**, *161* (3), A410−A415.
(33) Mizrahi, O.; Amir, N.; Pollak, E.; Chusid, O.; Marks, V.; Gottlieb, H.; Larush, L.; Zinigrad, E.; Aurbach, D. Electrolyte Solutions with a Wide Electrochemical Window for Recharge Magnesium Batteries. *J. Electrochem. Soc.* **2008**, *155* (2), A103−A109.
(34) Pour, N.; Gofer, Y.; Major, D. T.; Aurbach, D. Structural Analysis of Electrolyte Solutions for Rechargeable Mg Batteries by Stereoscopic Means and DFT Calculations. *J. Am. Chem. Soc.* **2011**, *133* (16), 6270−6278.
(35) Whittingham, M. S. Electrical Energy Storage and Intercalation Chemistry. *Science* **1976**, *192* (4244), 1126−1127.
(36) Amir, N.; Vestfrid, Y.; Chusid, O.; Gofer, Y.; Aurbach, D. Progress in Nonaqueous Magnesium Electrochemistry. *J. Power Sources* **2007**, *174* (2), 1234−1240.
(37) Prem Kumar, T.; Prabhu, P. V. S. S.; Srivastava, A. K.; Bejoy Kumar, U.; Ranganathan, R.; Gangadharan, R. Conductivity and Viscosity Studies of Dimethyl Sulfoxide (DMSO)-based Electrolyte Solutions at 25 °C. *J. Power Sources* **1994**, *50* (3), 283−294.

DOI: 10.1021/acsami.5b01206
ACS Appl. Mater. Interfaces 2015, 7, 7001−7007

(38) Carter, T. J.; Mohtadi, R.; Arthur, T. S.; Mizuno, F.; Zhang, R.; Shirai, S.; Kampf, J. W. Boron Clusters as Highly Stable Magnesium-Battery Electrolytes. *Angew. Chem., Int. Ed.* **2014**, *53* (12), 3173−3177.
(39) Suo, L.; Hu, Y.-S.; Li, H.; Armand, M.; Chen, L. A New Class of Solvent-in-Salt Electrolyte for High-Energy Rechargeable Metallic Lithium Batteries. *Nat. Commun.* **2013**, *4*, 1481.

DOI: 10.1021/acsami.5b01206
ACS Appl. Mater. Interfaces 2015, 7, 7001−7007